Voltage Instability Load Shedding

1012491

Voltage Instability Load Shedding

1012491

Technical Update, September 2006

EPRI Project Manager

P. Zhang

ELECTRIC POWER RESEARCH INSTITUTE
3420 Hillview Avenue, Palo Alto, California 94304-1395 • PO Box 10412, Palo Alto, California 94303-0813 • USA
800.313.3774 • 650.855.2121 • askepri@epri.com • www.epri.com

ORGANIZATION(S) THAT PREPARED THIS DOCUMENT

Electric Power Research Institute

This is an EPRI Technical Update report. A Technical Update report is intended as an informal report of continuing research, a meeting, or a topical study. It is not a final EPRI technical report.

NOTE

For further information about EPRI, call the EPRI Customer Assistance Center at 800.313.3774 or e-mail askepri@epri.com.

CITATIONS

This document was prepared by

Electric Power Research Institute
3420 Hillview Aveneu
Palo Alto, CA 94304

Principal Investigators
P. Zhang
L. Min
N. Zhang

This document describes research sponsored by the Electric Power Research Institute (EPRI).

This publication is a corporate document that should be cited in the literature in the following manner:

Voltage Instability Load Shedding. EPRI, Palo Alto, CA: 2006. 1012491.

REPORT SUMMARY

EPRI invented Voltage Instability Load Shedding (VILS) as a special protection scheme to prevent voltage collapse.

Background

Under Voltage Load Shedding (UVLS) has been used as an economic means of avoiding voltage collapse. The UVLS scheme is only used when all other means of avoid voltage collapse are exhausted. The UVLS scheme sheds load in pre-defined blocks that are triggered in stages when local voltage drops to various pre-defined levels. In most currently deployed UVLS schemes, voltage magnitude is the only triggering criteria. However, past research has demonstrated that voltage magnitude alone is not a satisfactory indicator of the proximity to voltage instability under all circumstances. In fact, voltage stability is determined by the power system's ability to supply and deliver reactive power. A new method is required to enhance the effectiveness of the Under Voltage Load Shedding (UVLS) scheme in both ensuring its safety net function and taking advantage of wide area coordination.

Objectives

This project aims at developing a new control scheme to enhance the conventional UVLS.

Approach

EPRI project team first reviewed the latest research and development work in UVLS area. Through this effort, the project team found the Voltage Instability Predictor (VIP) method. After having performed further investigation on the VIP method, the project team recognized the drawbacks of the VIP method. Thereafter, the project team developed the new voltage stability margin index and proposed using Kalman Filter to replace Least Square approach used in the VIP method. The project team named this invention as "Voltage Instability Load Shedding".

Results

A new control scheme named Voltage Instability Load Shedding has been developed to enhance the conventional UVLS. This smart control scheme uses local measurements to estimate voltage stability margin. When it detects that the voltage stability conditions cross a warning threshold, this smart device will send an alarm signal to inform system operators. When it detects that the voltage stability conditions cross an emergency level, it will perform local load shedding function. In addition, with wide application of this smart control devices across the transmission network, system operators can monitor system stability condition in a wide-area perspective.

EPRI Perspective

EPRI launched multi-year research efforts titled "Coordinated Wide-Area Voltage Instability Load Shedding Helps Prevent Voltage Collapse". This project, as the first step of the multiple-year research efforts, focuses on the theoretical investigation and methodology development on the VILS control scheme. The overall efforts aims at enhancing UVLS scheme, therefore, improving the reliability of the local and wide area transmission grid.

Keywords

Under Voltage Load Shedding
Voltage Stability Monitor and Control
Voltage Collapse
Voltage Instability Load Shedding
Voltage Stability Margin Index
Wide-area Protection and Control

ABSTRACT

A new control scheme named Voltage Instability Load Shedding (VILS) has been developed to enhance the conventional UVLS scheme at designated locations (such as major load centers). This smart control scheme computes Voltage Stability Margin Index (VSMI) continuously to track the voltage stability margin at local bus level. The VSMI expressed as active, reactive, and apparent power is used as an adaptive triggering criterion for load shedding. This VILS control scheme comprises the steps of, or means for, measuring current and voltage waveforms at the local load bus, therefrom estimating Thevenin equivalent admittance (Y), then calculating the VSMI, and finally comparing the VSMI with the pre-set threshold to decide whether to initiate a load shedding action.

CONTENTS

LIST OF FIGURES

LIST OF TABLE

1 INTRODUCTION

A power systems are pushed to transfer more and more power, voltage stability now becomes a major concern in planning and operating electric power systems. Load increases and/ or generation rescheduling stress the system by increasing power transfer over long distances and/ or by drawing on reactive power reserves. It is critical to track how close the transmission system is to its loadability limit. If the loading is high enough, actions (such as load shedding) have to be taken to relieve the transmission system. A problem associated with tracking the loadability limit of the transmission system is that such limit is not a fixed quantity, but rather depends on the network topology, generation and load patterns, and the availability of VAR resources. All of these factors can vary with time due to scheduled maintenance, unexpected disturbances, etc.

There is still a need at the local substation level to mitigate local voltage instability. The function can be incorporated into the protective relays that only use local measurements. These relays will only be operated when other controls can not mitigate the aggravating situation. They also form the fall-back position for any global protection scheme when communication channels fail. Control schemes that only use local data provide an attractive approach because they are fast, low cost and simple to build. The most common form is to shed load based on voltage level – Under Voltage Load shedding (UVLS) [1].

Under Voltage Load Shedding scheme is receiving attention as a means of avoiding voltage collapse. This scheme is only used when all other means of avoiding voltage collapse are exhausted. Since load shedding results in high costs to electricity suppliers and consumers, Under-Voltage Load Shedding (UVLS) schemes have been deployed as a ‘Safety Net’ to prevent voltage collapse following an extreme event. UVLS sheds load in pre-defined blocks that are triggered in stages when local voltage drops to various pre-defined levels.

Tuan etc [2] proposed a load shedding algorithm that is based on the indicators of risk of voltage instability and on the sensitivities of these indicators to the changes of loads to be shed. However, the analysis is based on the static models and the dynamic aspects associated with voltage stability are not taken into account. Tso et al. [3] presented a load shedding scheme taking into account the generator dynamics. The load shedding scheme is based on extended fuzzy reasoning. However, the amount of load to be shed is fixed. Arnborg et al [4] proposed a method for UVLS. The method took into account the generator and load dynamics and focused on long-term voltage stability, assuming the generator transients have settled when the load dynamics are dominating. A UVLS criterion was developed using a dynamic load model. Their studies showed that an iterative load shedding scheme could be successful in avoiding voltage collapse.

In those proposed UVLS schemes, voltage magnitude is the only triggering criteria. However, past research has demonstrated that voltage magnitude alone is not a satisfactory indicator of the proximity to voltage instability under all circumstances. In fact, voltage stability is determined by the power systems’ ability to supply and deliver reactive power. In actual systems, the computation of actual system PV curves may be very complicated due to the large number of generators, the widespread applications of capacitor banks, the uncertainty about the dynamic characteristics of system loads, and the variability of power flow pattern. In addition, operation of under load tap changers, the actual dynamic reactive capability of generators and accurate reactive reserve monitoring all affect the ability of the system to supply and deliver the reactive power.

Currently, settings of UVLS are determined by system engineers through extensive network analyses using computer simulation packages. However, simulated system behaviors do not usually coincide with actual measured system responses due to data and modeling issues. Developing appropriate settings for the under voltage levels and time delays are challenging problems faced by system engineers. Inappropriate settings can result in unnecessary shedding or failure to detect the need for load shedding.

After having recognized this challenge, EPRI launched a multiple year research efforts titled “Coordinated Wide-Area Voltage Instability Load Shedding Helps Prevent Voltage Collapse”. The overall efforts aims at enhancing under-voltage load shedding design, therefore, improving the reliability of the local and wide area transmission grid. As a result, a new control scheme named “Voltage Instability Load Shedding” has been invented. This report summarizes the theoretical investigation and methodology development on the VILS scheme.

This report is organized as follows: Section 2 reviews the voltage instability predictor (VIP) method. In Section 3, a new voltage stability margin index is proposed for VILS and IEEE test systems are used to demonstrate the proposed method. Section 4 describes and compares two estimation methods to track the Thevenin equivalent: Least Square techniques and Kalman Filter techniques. Section 5 summarizes the research results and presents the future work.

2 VOLTAGE INSTABILITY PREDICTOR METHOD

Vu and Begovic et al.[5] have proposed Voltage Instability Predictor (VIP) method to estimate the proximity of a power system to voltage collapse. The VIP only uses the local measurements (voltage and current) at the bus terminal to estimate the Thevenin impedance and calculate the apparent impedance of local load, then detects the proximity to voltage collapse by monitoring the relationship between those two impedances.

2.1 Voltage Instability Predictor Method

Figure 2-1 shows a load bus and the rest of the system treated as a Thevenin equivalent.

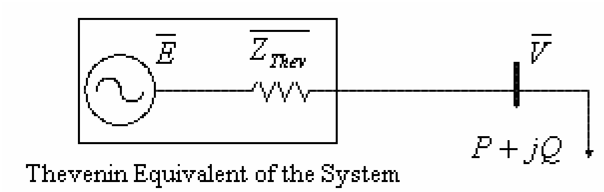

Figure 2-1
Local bus and the rest of the system treated as a Thevenin equivalent.

Equating the receiving and sending currents, we have

$$\begin{aligned} &\frac{P + jQ}{\overline{V}} = \overline{I}^* = \left(\frac{\overline{E} - \overline{V}}{\overline{\overline{Z}}_{Thev}}\right)^* \\ &\Rightarrow (P + jQ) \cdot \overline{Z}^*_{Thev} = \overline{V}\left(\overline{E} - \overline{V}\right)^* \end{aligned} \tag{2-1}$$

For a given power transfer $P+jQ$, there at most two voltage solutions. Observing the symmetry in Equation (2-1), we can find that, if $\overline{V}$ is one solution then the other solution can be found simply by computing $\left(\overline{E} - \overline{V}\right)^*$. As the load increases to the maximum value, the two solutions become one. Further increase in load will yield no solution. In summary, the maximum power transfer happens when $\overline{V} = (\overline{E} - \overline{V})^*$

$$\text{Maximal power transfer } \Leftrightarrow \overline{V} = (\overline{E} - \overline{V})^* \tag{2-2}$$

Therefore,

$$\text{Maximal power transfer} \Leftrightarrow \overline{Z}_{app}\,\overline{I} = (\overline{Z}_{Thev}\,\overline{I})^* \tag{2-3}$$

Finally,

$$\text{Maximal power transfer} \Leftrightarrow \left|\overline{Z}_{app}\right| = \left|\overline{Z}_{Thev}\right| \tag{2-4}$$

Tracking closeness to voltage instability, therefore, becomes tracking the distance of the present-time apparent impedance $\left|\overline{Z}_{app}\right|$ to the Thevenin circle, as shown in Fig. 2-2. This circle is by no means a fixed object because it represents the rest of the system lumped together. Such collection involves thousands of equipments, any of which can change at a given time. More likely, when approaching to voltage instability, the circle expands (transmission system becoming weaker) and the impedance $\left|\overline{Z}_{app}\right|$ moves toward it (load becoming heavier).

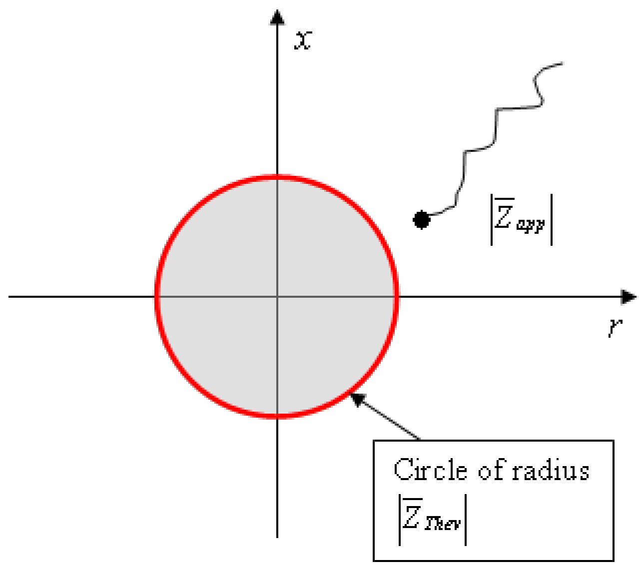

Figure 2-2
Maximal power transfer (voltage instability) is reached when the apparent impedance of the load bus hits the Thevenin circle.

2,2 Implementation of VIP

The flowchart depicted in Fig. 2-3 summarizes the process of the VIP method.

Step 1: The measurement of voltage and current samples are acquired at the local bus.

Step 2: Calculate the voltage and current phasor.

Step 3: Te local load apparent impedance $\left|\overline{Z}_{app}\right|$ can be calculated using measured voltage and current. The Thevenin equivalent impedance $\left|\overline{Z}_{Thev}\right|$ can be estimated using the Least Square method.

Step 4: $\left|\overline{Z}_{app}\right|$ and $\left|\overline{Z}_{Thev}\right|$ are then compared with the threshold, ε , to determine whether load shedding or other action should be taken.

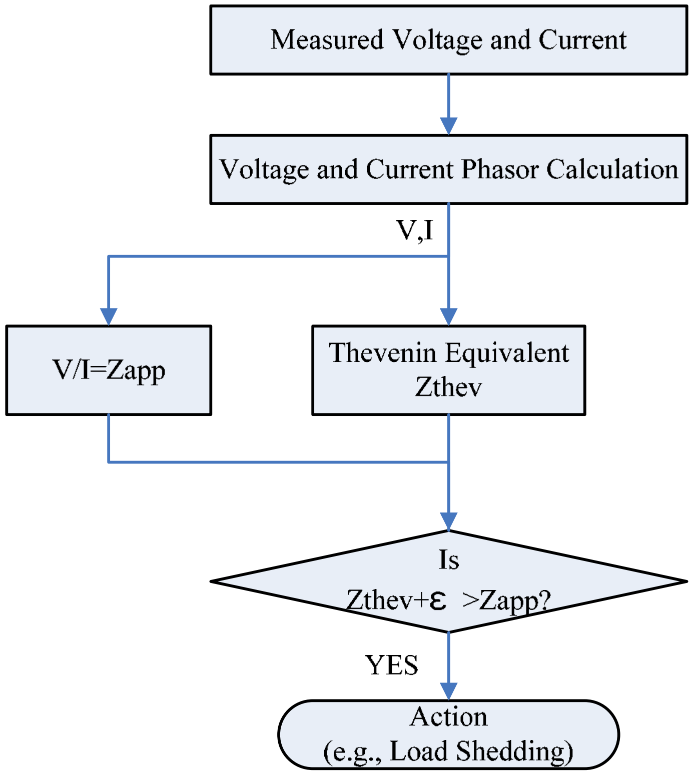

Figure 2-3
The process of VIP method

2.3 Use of VIP algorithm in Load Shedding

In order to make the algorithm practical, it is necessary to act on the conservative side. That is, one should set a margin and the device acts when the margin is violated. The choice of margin, of course, depends on the bus; it also involves heuristics. For example as Fig. 2-4, one may want to set the margin for a certain bus to be 0.15 (per unit impedance); with this choice, the voltage collapse is “detected” when the load reaches 125%. Thus, the load at this bus is deemed excessive when the power margin is violated. Load can be shed so as to restore the margin. Clearly, the amount of load to be shed is not fixed and thus, VIP algorithm provides a form of adaptive load shedding.

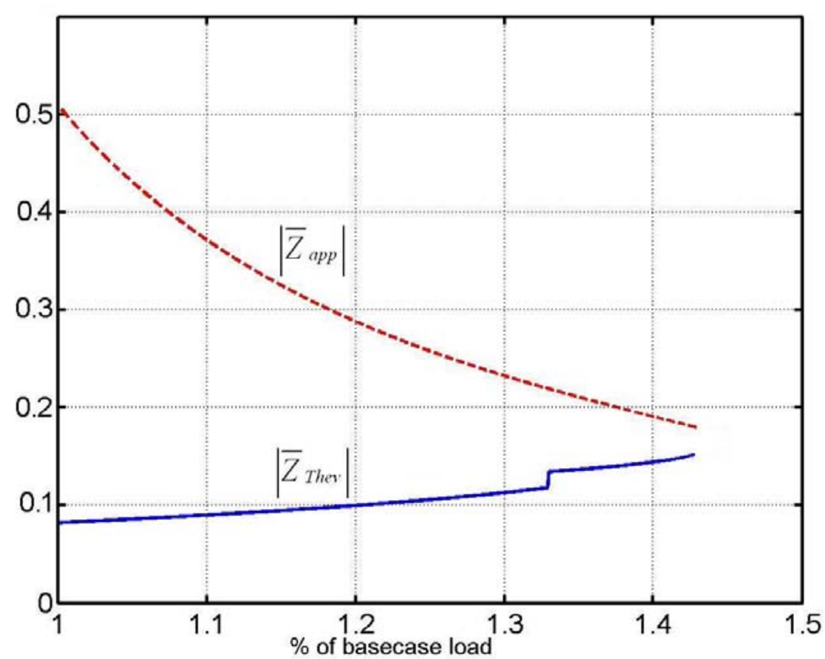

Figure 2-4
Maximal power transfer is reached (voltage instability) when the apparent impedance of the load bus hits the Thevenin circle.

VIP method indicates that, at the point of maximum loading, the absolute value of the apparent load impedance and the equivalent Thevenin impedance are equal. Based on the closeness between those two impedances, VIP method will determine whether need to shed load. However, VIP method does not provide any information about how much load should be shed in order to bring the system back to voltage stable. Moreover, VIP method uses the Least Square technique to determine the Thevenin equivalent impedance. The Least Square technique makes use of measurements taken at different time instant to estimate the equivalent source impedance. Protective relay impedance comparators have been able to estimate the source impedance with some accuracy during faults, but this is primarily due to the fact that there is a significant difference in measurements between pre- and post-fault conditions. During power swings, this is not necessarily the case, and unless the measurements have changed sufficiently from one measurement to the next, the accuracy of the Least Square technique may be questionable.

3 VOLTAGE INSTABILITY LOAD SHEDDING

We propose an innovative control scheme named “Voltage Instability Load Shedding” (VILS) to enhance traditional UVLS scheme. VILS method computes Voltage Stability Margin Index (VSMI), which express voltage stability margin in terms of active, reactive, and apparent power, in order to continuously track the voltage stability margin at local bus level. Compared with the VIP method, VILS method can determine how much loads need to be shed at local bus level in order to prevent voltage instability or collapse.

3.1 Voltage Stability Margin Index

For the Thevenin Equivalent system as shown in Figure 2-1, we derived an analytical expression of the critical condition of static voltage stability in power injection space.

The real and reactive power transferred from the system to the load is

$$\begin{cases} P_L = EVY\cos(\alpha-\delta-\beta) - V^2 G \\ Q_L = EVY\sin(\alpha-\delta-\beta) + V^2 B \end{cases} \tag{3-1}$$

where Y is the magnitude and β is the angle of the series admittance $G + jB$.

Dividing E^2Y on both sides of Equation (1), it can be reformulated as:

$$\begin{cases} p = v\cos(\alpha-\delta-\beta) - v^2\cos\beta \\ q = v\sin(\alpha-\delta-\beta) + v^2\sin\beta \end{cases} \tag{3-2}$$

where $p = \dfrac{P_L}{E^2Y}, q = \dfrac{Q_L}{E^2Y}, v = \dfrac{V}{E}$

Moving $v^2\cos\beta$ and $v^2 sin\beta$ to the left sides and taking the square of the right and left sides and adding, the following equation is obtained:

$$(p + v^2\cos\beta)^2 + (q - v^2 sin\beta)^2 = v^2 \tag{3-3}$$

Substitute q with $p \cdot \tan\phi$ where ϕ is the power factor. From equation (3-3), we can get:

$$p = -v^2\cos\phi\cos(\phi+\beta) + \cos\phi\sqrt{v^2 - v^4\sin^2(\phi+\beta)} \tag{3-4}$$

Taking the derivative and setting it equal to zero, we get the normalized critical voltage and the maximum power.

$$\frac{\partial p}{\partial v} = 1 - 4v^2 + 4v^4\sin^2(\phi+\beta) = 0 \tag{3-5}$$

$$v_{critical}{}^{2} = \frac{1-\cos(\phi+\beta)}{2\sin^{2}(\phi+\beta)} = \frac{1}{2[1+\cos(\phi+\beta)]} \tag{3-6}$$

$$p_{\max} = \frac{\cos\phi}{2[1+\cos(\phi+\beta)]} \tag{3-7}$$

The maximum active and reactive transfer power can be obtained as:

$$\begin{aligned} P_{\max} &= E^{2}Y \cdot p_{\max} = V^{2}Y\cos\phi \\ Q_{\max} &= E^{2}Y \cdot Q_{\max} = V^{2}Y\sin\phi \end{aligned} \tag{3-8}$$

Therefore, as shown in Fig. 3-1, tracking closeness to voltage instability becomes tracking the distance of the current load level to the maximum power transfer point.

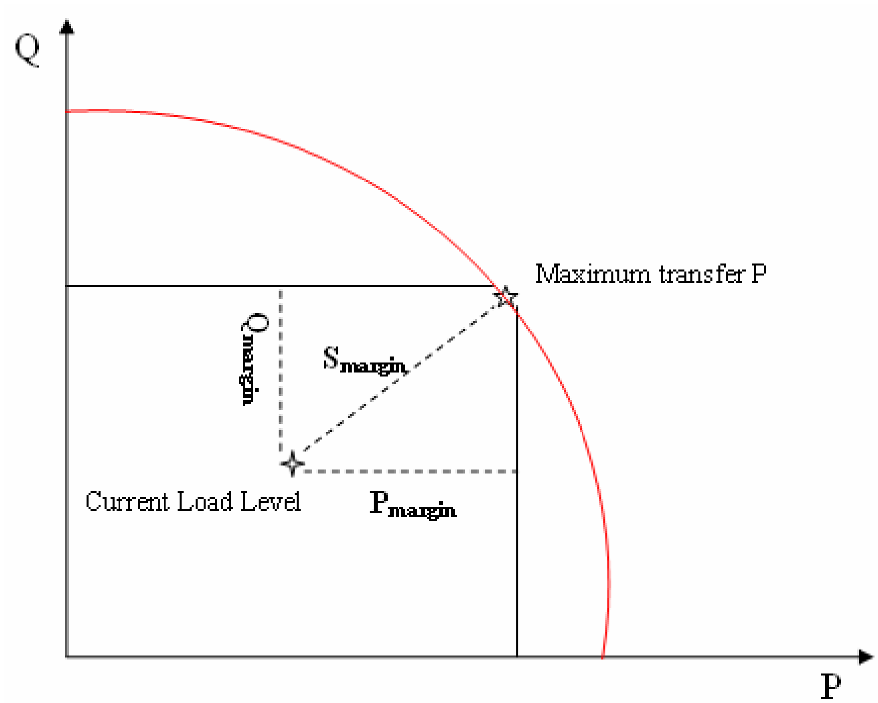

Figure 3-1
Voltage Stability Margin is expressed in P and Q plane. Tracking closeness to voltage instability becomes tracking the distance of the current load level to the maximum power transfer point.

As illustrated by Equations (3-9 ~ 3-11), the VSMI can be expressed in terms of the apparent, active and reactive power. The closer the margins are to zeros, the more imminent is the voltage instability.

VSMI in terms of active power:

$$P_{Margin} = P_{\max} - P_{L} \tag{3-9}$$

VSMI in terms of reactive power:

$$Q_{Margin} = Q_{max} - Q_L \tag{3-10}$$

VSMI in terms of apparent power:

$$S_{Margin} = P_{\max} + jQ_{\max} - S_L \tag{3-11}$$

The maximum transfer power point is by no means a fixed object. As the system approaches voltage instability, the maximum transfer power point and the current load level moves toward each other.

The VILS method provides the load shedding information in the injection plane instead of the impedance plane. Displaying the voltage stability margin in the power injection space provides voltage stability margin in terms of MW, MVar and MVA. As a result, it not only judges whether load shedding action should be taken place but also provides the information about how much loads need to be shed.

In addition, according to Equation (3-8), we can obtain that

$$P_{\max}^2 + Q_{\max}^2 = (V^2 Y)^2 \tag{3-12}$$

Due to this relationship between Pmax and Qmax, the voltage stability margin boundary for a given network configuration is shown as the red line in Figure 3-2. This boundary is independent of local load characteristic, in particular the power factor of load.

3.2 Voltage Instability Load Shedding

To apply VSMI to VILS, a stability margin ε is set as the threshold and the load shedding acts when the threshold is violated for a certain time. The flowchart depicted in Fig. 3-2 summarizes the process of VILS.

Step 1: The voltage and current at load bus are measured.

Step 2: Calculate the voltage and current phasor.

Step 3: Calculate the local real and reactive power load P_L and Q_L can be calculated. Thevenin equivalent admittance Y can be estimated using the Kalman Filter method described in the next Section.

Step 4: The voltage phasor and estimated Thevenin equivalent admittance are used to predict the maximum power load at this operating point by using equation (3-8).

Step 5: With the predicted maximum transfer power and the local load, Pmargin/Qmargin/Smargin can be calculated by using equation (3-9, 3-10, 3-11). These margins, then, compared with the user defined threshold, ε, to determine whether the load shedding or other action should be taken.

Step 6: If the calculated margin is large than ε, which means that the system is voltage stable. If the calculated margin is less than ε, which means that the system is close to the voltage instability point, the load shedding action should be taken place to restore the margin.

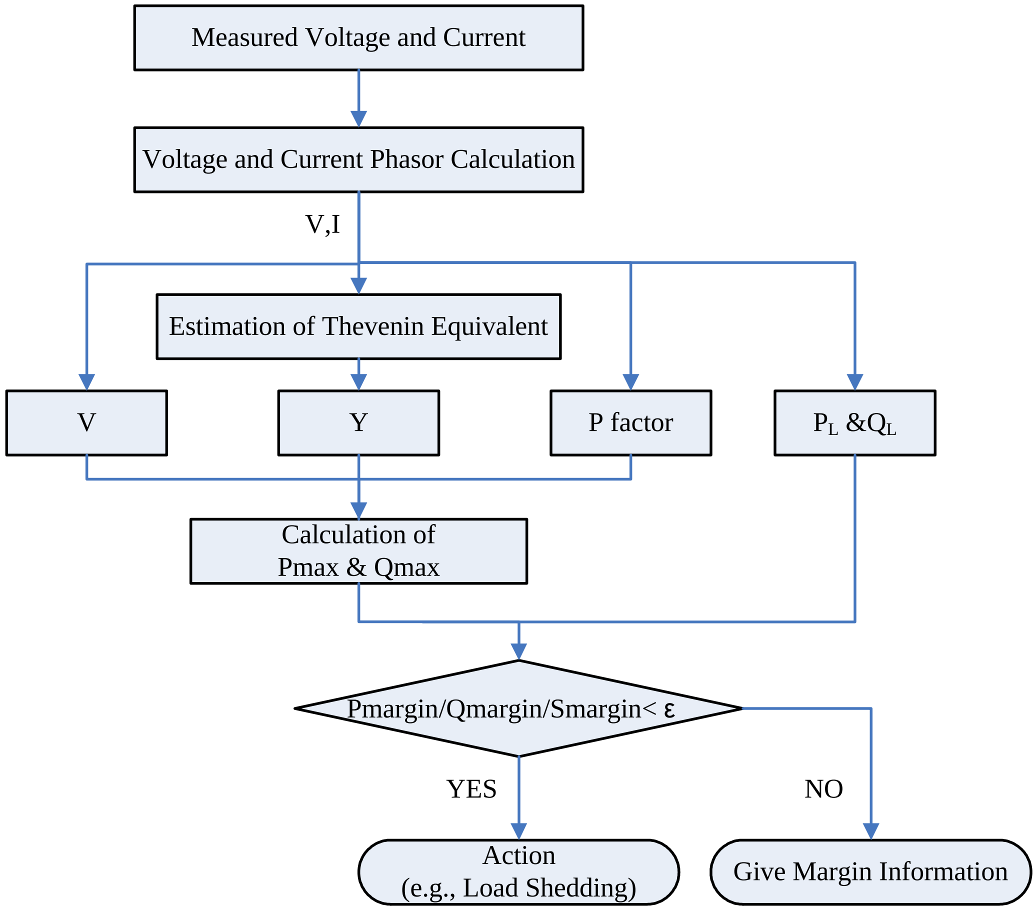

Figure 3-2
A flowchart of the operation of the Voltage Instability Load Shedding algorithm.

3.3 Illustrative Example

3.3.1 IEEE 39-Bus System

IEEE 39-Bus system is the equivalent system of New England transmission network. Figure 3-3 shows the system diagram. For the steady state simulation, the iterative power flow program is used to simulate the voltage instability phenomenon.

- The base load at Bus 26 is 139+j17 MVA.
- Gradually increase load at bus 26, 27, 28 and 29 at10 MW per step.
- Reactive power increases correspondingly according to the base case P/Q ratio.
- Governor power flow is used to calculated generators' output in order to balance the increasing load.
- Generator reactive power output limits are also considered.
- The simulation ends when the power flow calculation failed to converge.

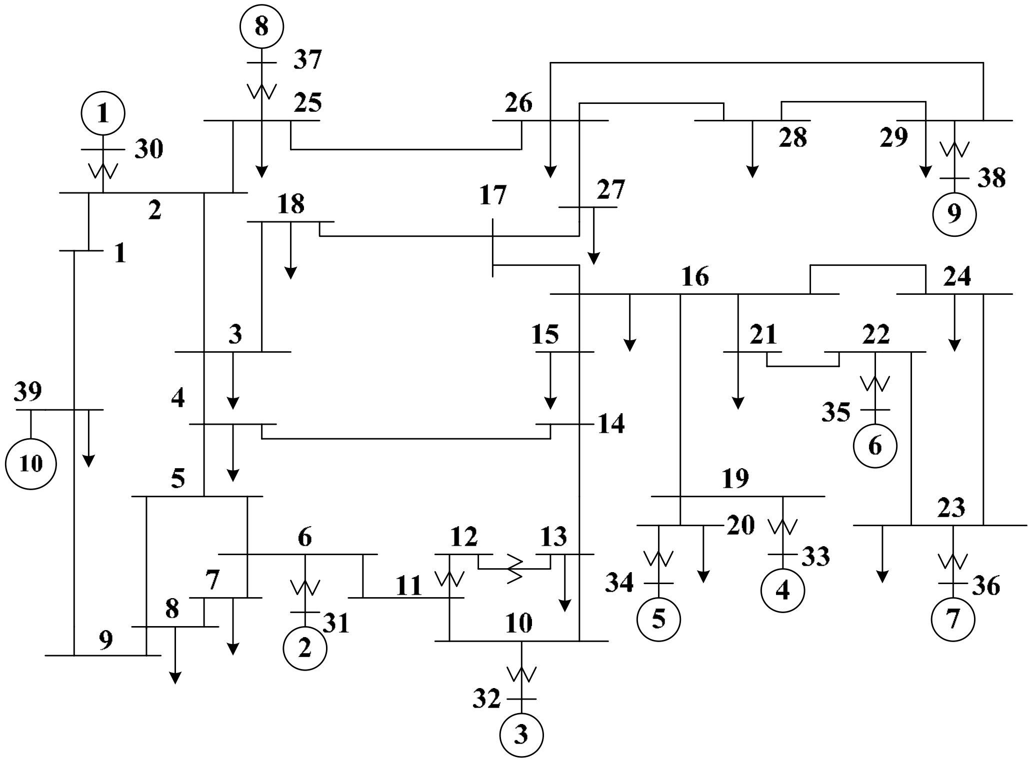

Figure 3-3
IEEE 39-bus System

Governor Power Flow:

Governor power flow allows governor distribution of the mismatch caused by increasing loads. All generators will participate in proportional to their governor gains.

$$G(i) = \frac{C_i}{\sum_{i=1}^{M} C_i} \tag{3-12}$$

where
M is the generator number;
Ci is the MW capacity of generator *i*;

The governor gain can be calculated as:

$$G(i) = \frac{\beta_i}{\sum_{i=1}^{M} \beta_i} \tag{3-13}$$

where β_i is the frequency response characteristic of generator i;

$$\beta_i = \frac{C_i}{\omega_0 R} \tag{3-14}$$

where
ω_0 is the nominal system frequency in redians/second;
R is the system regulation coefficient (R = 0.5).

The generator MW capacities and their governor gains are listed in Table3-1.

Table 3-1
MW capacity of generators and governor gains

	G30	G31	G32	G33	G34	G35	G36	G37	G38
MW Capacity	350	1145.55	750	732	608	750	660	640	930
Governor Gain	0.0533	0.1745	0.1142	0.1115	0.0926	0.1142	0.1005	0.0975	0.1416

Generator Reactive Power Output Limits:

Generator VAR output limits are considered in the simulation. The reactive power limits are set as the half value of the generators' active power capacities. The iterative power flow is used to compute the PV curves. Table 3-2 summarizes the voltage magnitude and VAR output of generator buses at the critical point. The PV curves at bus 26 with and without VAR limit are shown in Fig.3-4. Table 3-3 compares the active power and the voltage magnitude of bus 26 at the critical point between with and without consideration of reactive power limits. From Table 3-3, we can see that system with consideration of generators VAR limits will reach voltage instability point earlier than the ones without considering generators VAR limits.

Table 3-2
Generator bus voltage and VAR output

	Voltage Magnitude	Var Output (MVAR)	VAR Limit (MVAR)	Reach VAR limit?
Bus 30	0.9850	175	175	Y
Bus 31	0.9820	565.5	572.8	N
Bus 32	0.9692	375	375	Y
Bus 33	0.9972	328.9	366	N
Bus 34	1.0123	275.3	304	N
Bus 35	1.0347	375	375	Y
Bus 36	1.0635	285.1	330	N
Bus 37	0.9818	320	320	Y
Bus 38	1.0265	465	465	Y

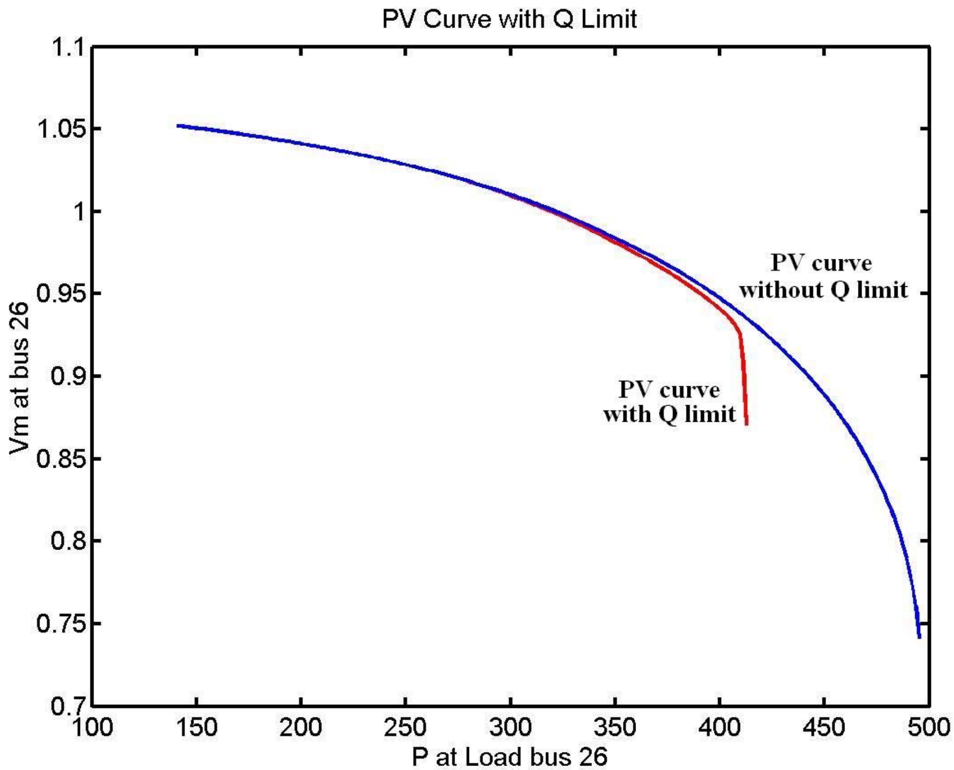

Figure 3-4
Comparison of PV curves at bus 26 with and without VAR limits

Table 3-3
Critical points with and without VAR limit

	Without VAR Limit		With VAR Limit	
Bus 26	MW at bus 26	VM at bus 26	MW at bus 26	VM at bus 26
	495.10	0.7410	412.57	0.8703

Figure 3-5 shows voltage stability margin in P-Q plane. The voltage stability limit is shown as the green curve in Figure 3-6. The current active power of the load at bus 26 is 261.3 MW. At this point, the P margin and Q margin are 844.2 MW and 103 MVar respectively.

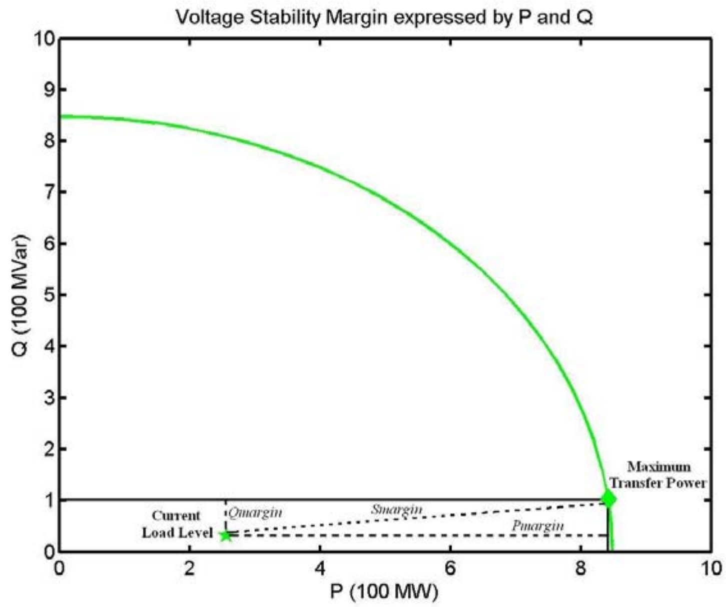

Figure 3-5
Voltage stability margin in terms of P and Q

Figure 3-6 shows that, as the local load at bus 26 increases, the voltage stability margin will shrink.

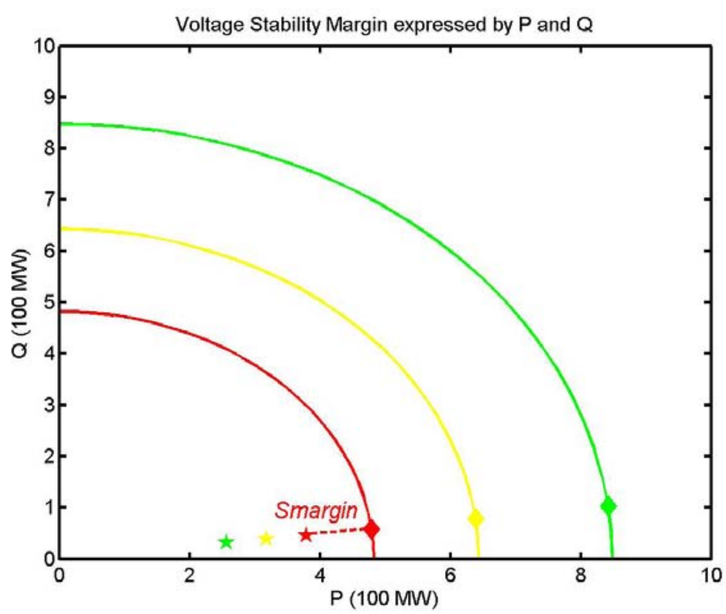

Figure 3-6
Voltage stability margin circle changes

Figure 3-7 shows the voltage stability margin as a function of local load at bus 26. It is clearly indicates that as the load at bus 26 increase, the voltage stability margin will decrease.

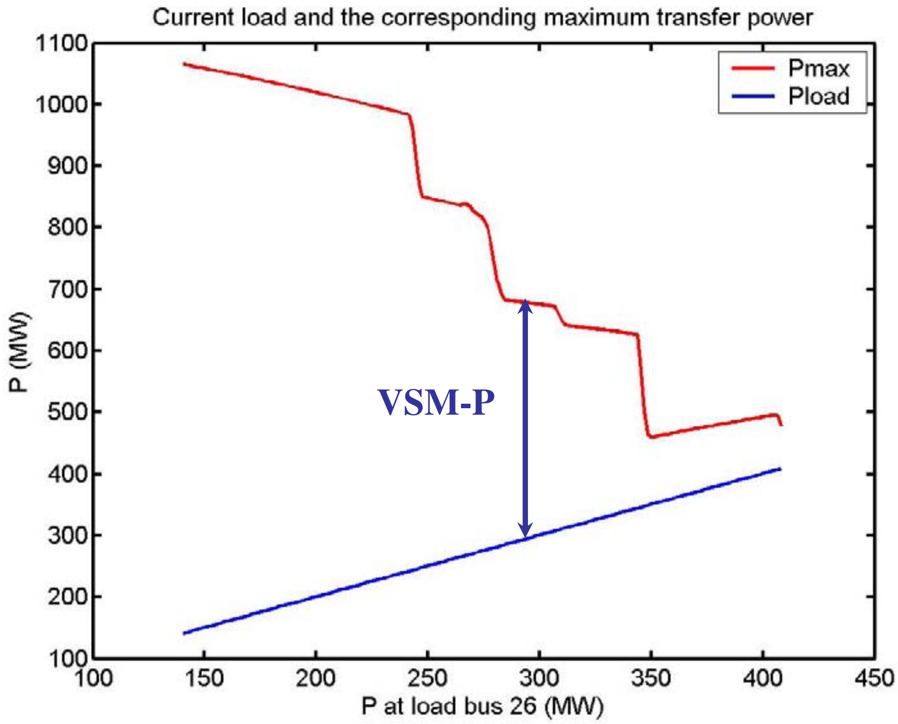

(a) Voltage Stability Margin in terms of P

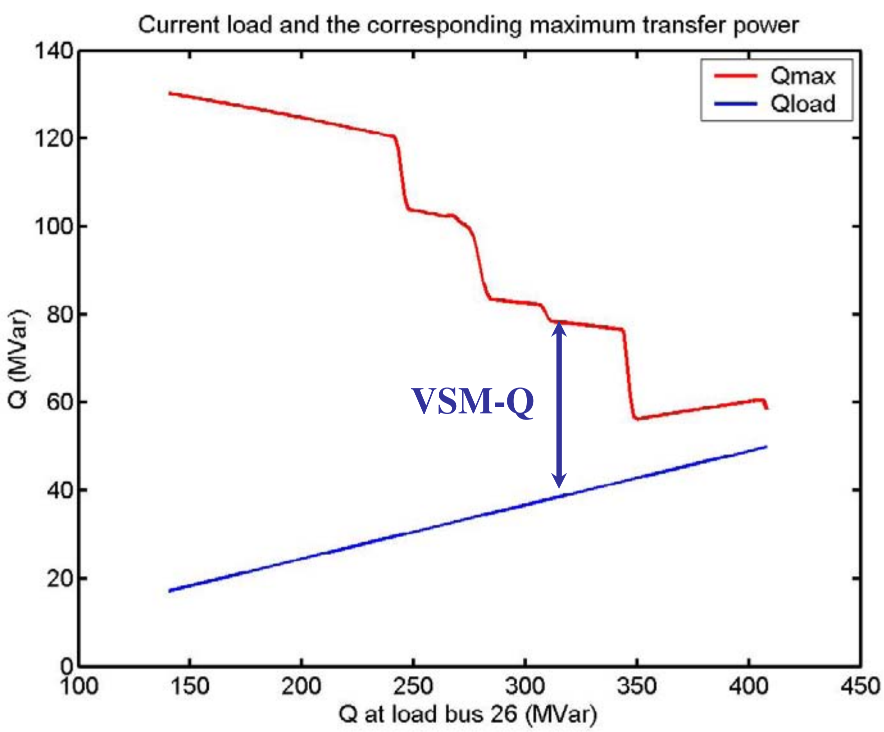

(b) Voltage Stability Margin in terms of Q

Figure 3-7
Voltage stability margin as a function of local load at bus 26

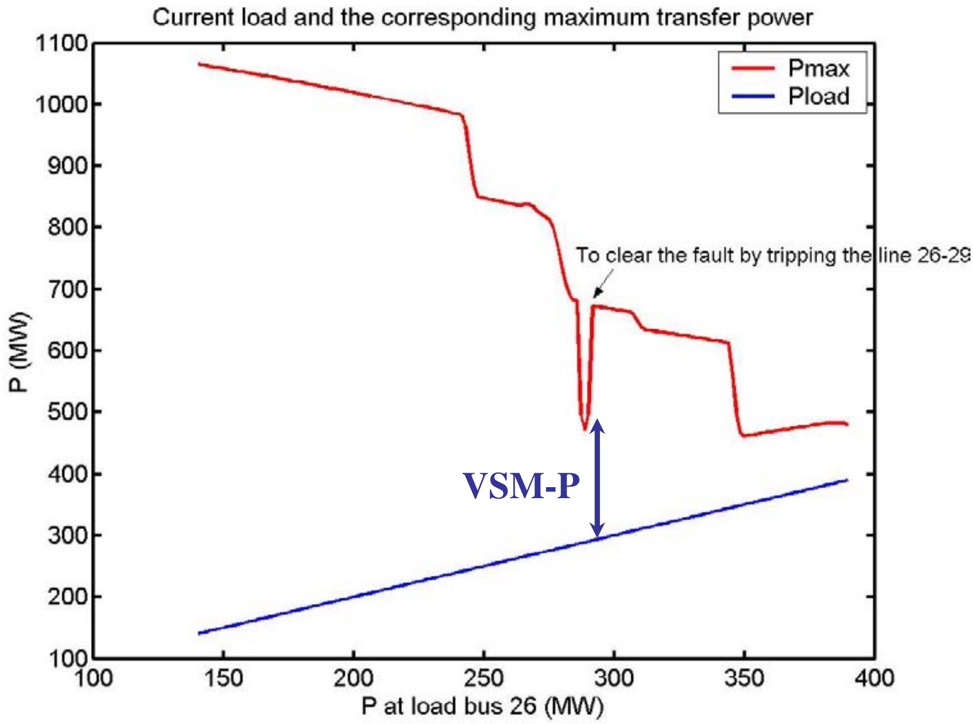

(a) Do not block

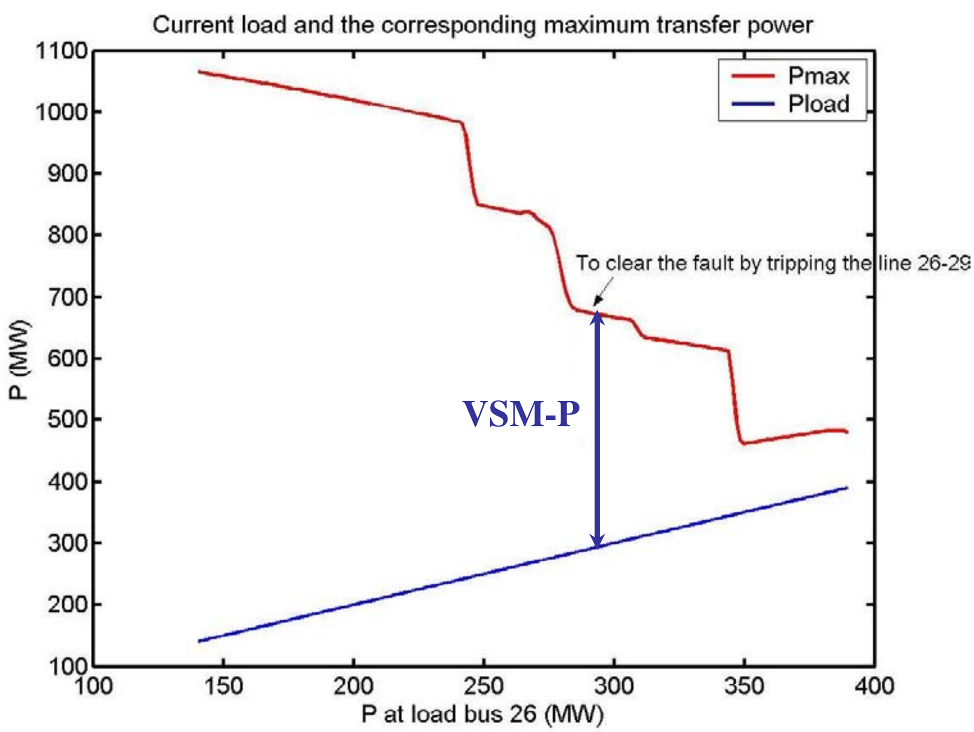

(b) Block 30 circles during the fault condition

Figure 3-8
voltage stability margin during fault

We also analyzed the voltage stability margin during a fault. A fault at bus 26 is simulated with line 26-29 tripped to clear the fault. Figure 3-8 (a) shows the voltage stability margin without blocking the fault during the simulation and Figure 3-8 (b) shows the voltage stability margin with blocking the fault during the simulation. Because voltage stability margin reduce dramatically during the transient stage and could potentially lead to misoperation of VILS, we suggest that VILS should be blocked during the transient stages.

3.3.2 IEEE 118-Bus system

IEEE 118-Bus system is the equivalent system of a portion of the American Electric Power transmission network in Midwestern of US. Figure 3-9 shows the one-line diagram. Table 3-4 shows the partition of this system. Lists case is a transaction between area 2 and area 1.

- The load at Bus 22 in base case is 10+j5 MVA.
- The total load in area 1 increase 5 MW per step.
- The reactive power of load in area 1 increases correspondingly according to the power factor defined in the base case.
- Governor power flow is used to calculated generators' output in order to balance the increasing load.
- Generator reactive power output limits are also considered.
- The simulation ends when the power flow calculation failed to converge.

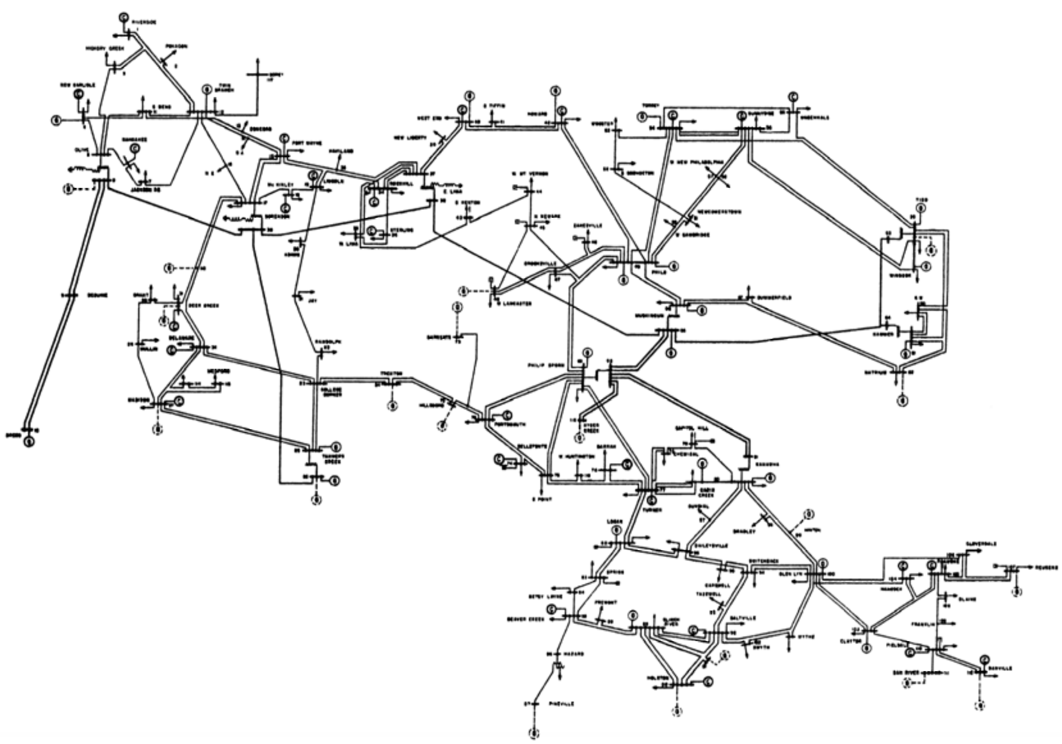

Figure 3-9
IEEE 118-Bus System

Table 3-4
Partitioned IEEE 118-bus system

Area/Lines			Area/Buses		
Area 1	Area 2	Area 3	Area 1	Area 2	Area 3
1~29 31~43 178~182 184	46~53 55~107 183	109~115 117~118 120~125 127~177 185~186	1~23 25~32 113~115 117	33~69 116	24 70~112 118

Figure 3-10 shows the voltage stability margin as a function of local load at bus 22. It is clearly indicates that as the load at bus 22 increase, the voltage stability margin will decrease.

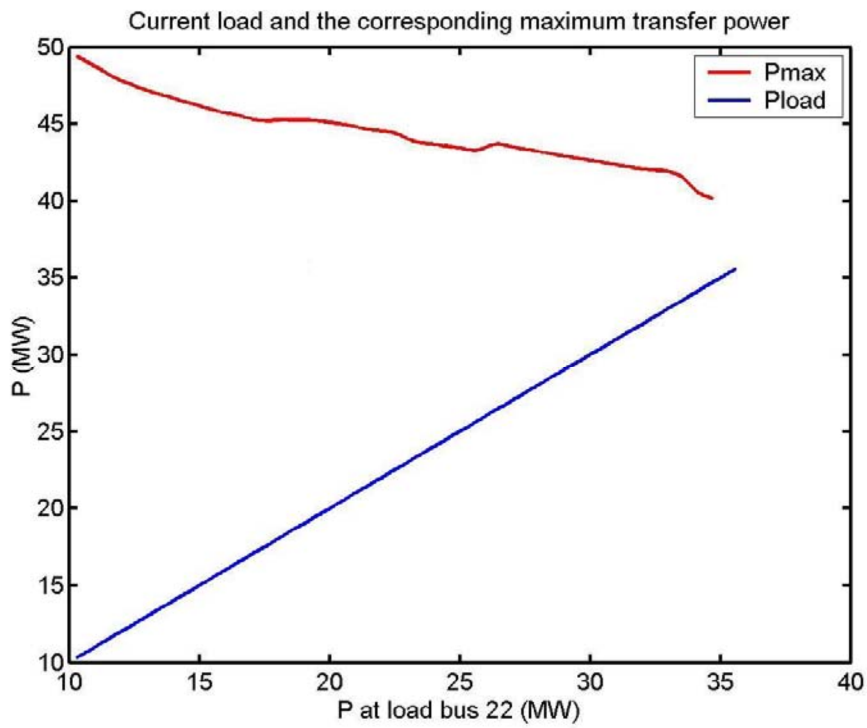

(a) Voltage Stability Margin in terms of P

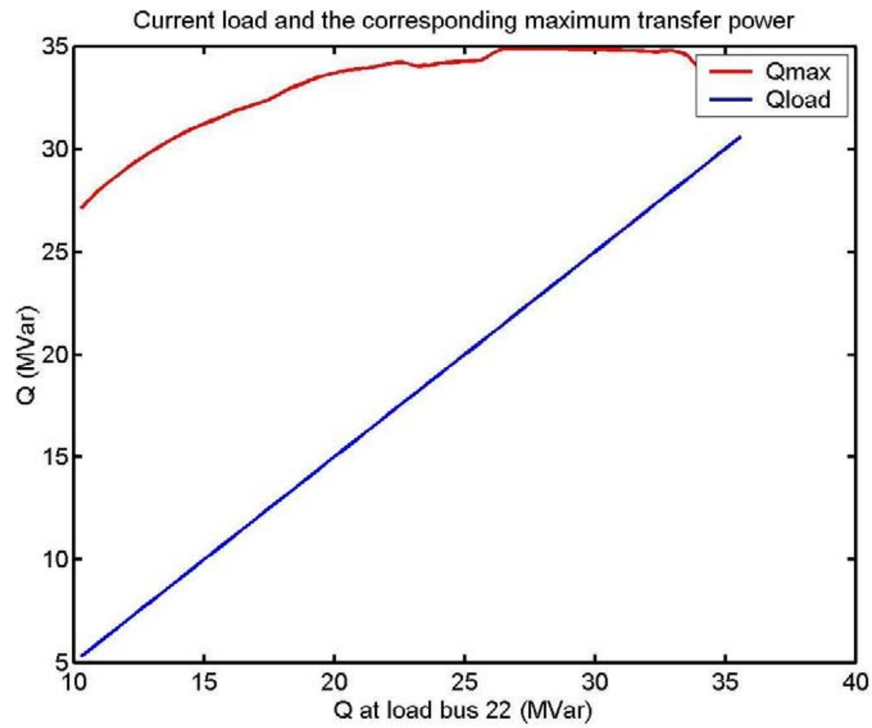

(B) Voltage Stability Margin in terms of Q

Figure 3-10
Voltage stability margin as a function of local load at bus 22

4 THEVENIN EQUIVALENT ESTIMATIION TECHNIQUES

4.1 Introduction

VILS control scheme requires estimating the Thevenin Equivalent using local measurements. This chapter will describe and compare two estimation techniques: Least Square approach and Kalman Filter approach.

4.2 Calculation of the Actual Thevenin Equivalent

If the entire system data is known, the actual Thevenin Equivalent at load bus can be calculated. The calculated actual Thevenin Equivalent value is used as the benchmark to verify the accuracy of the estimation approaches.

$$YU = I \tag{4-1}$$

where U is a vector of voltage magnitude, I is a vector of current injection, Y is admittance matrix. Y is $n \times n$ matrix, U is $n \times 1$, I is $n \times 1$, where n is the number of buses.

Suppose we want to obtain the Thevenin Equivalent at Bus p. Move the row and column of Bus p to the last row and last column. The U and I are bus voltage vector and injection current vector.

$$\begin{bmatrix} Y_{11} & Y_{12} & \cdots & Y_{1n} & Y_{1p} \\ Y_{21} & Y_{22} & \cdots & Y_{2n} & Y_{2p} \\ \vdots & \vdots & & \vdots & \vdots \\ Y_{n1} & Y_{n2} & \cdots & Y_{nn} & Y_{np} \\ Y_{p1} & Y_{p2} & \cdots & Y_{pn} & Y_{pp} \end{bmatrix} \begin{bmatrix} U_1 \\ U_2 \\ \vdots \\ U_n \\ U_p \end{bmatrix} = \begin{bmatrix} I_1 \\ I_2 \\ \vdots \\ I_n \\ I_p \end{bmatrix} \tag{4-2}$$

Representing Equation (4-2) as following:

$$\begin{bmatrix} Y_{NN} & Y_{Np} \\ Y_{pN} & Y_{pp} \end{bmatrix} \begin{bmatrix} U_N \\ U_p \end{bmatrix} = \begin{bmatrix} I_N \\ I_p \end{bmatrix} \tag{4-3}$$

where Y_{NN} is a $(n-1) \times (n-1)$ matrix, Y_{Np} is a $(n-1) \times 1$ matrix, Y_{pN} is a $1 \times (n-1)$ matrix.

Eliminate the first n column and row by Kron's reduction.

$$\tilde{Y}_{pp} U_p = \tilde{I}_p \tag{4-4}$$

where $\tilde{Y}_{pp} = Y_{pp} - Y_{pN} Y_{NN}^{-1} Y_{Np}$ is the Norton equivalent admittance, $\tilde{I}_p = I_p - Y_{pN} Y_{NN}^{-1} I_N$ is the Norton equivalent source current.

Then Thevenin Equivalent at Bus *p* can be expressed as:

$$Z_{Thev} = \frac{1}{\tilde{Y}_{pp}} \tag{4-5}$$

$$E_{Thev} = Z_{Thev} \tilde{I}_p \tag{4-6}$$

4.3 Estimation of the Thevenin Equivalent using Least Square Method

Based on the Thevenin Equivalent diagram as shown in Figure 3-1,

$$\overline{E} = \overline{V} + \overline{Z_{Thev} I} \tag{4-7}$$

Denote $\overline{E} = E_r + jE_i$, $\overline{V} = u + jw$ and $\overline{I} = g + jh$.

Equation (4-6) is rewritten as:

$$\begin{bmatrix} 1 & 0 & -g & h \\ 0 & 1 & -h & -g \end{bmatrix} \times \begin{bmatrix} E_r \\ E_i \\ R_{Thev} \\ X_{Thev} \end{bmatrix} = \begin{bmatrix} u \\ w \end{bmatrix} \tag{4-8}$$

Note that *g*, *h*, *u* and *w* can be calculated, using local measurements. The unknowns are R_{Thev}, X_{Thev} and E_r and E_i. Since there are four unknown variables and two equations, two or more measurements are required to solve the unknowns.

For example, if we have three measurements, (4-8) can be rebuilt as:

$$\underbrace{\begin{bmatrix} 1 & 0 & -g_1 & h_1 \\ 0 & 1 & -h_1 & -g_1 \\ 1 & 0 & -g_2 & h_2 \\ 0 & 1 & -h_2 & -g_2 \\ 1 & 0 & -g_3 & h_3 \\ 0 & 1 & -h_3 & -g_3 \end{bmatrix}}_{A} \times \underbrace{\begin{bmatrix} E_r \\ E_i \\ R_{Thev} \\ X_{Thev} \end{bmatrix}}_{C} = \underbrace{\begin{bmatrix} u_1 \\ w_1 \\ u_2 \\ w_2 \\ u_3 \\ w_3 \end{bmatrix}}_{B} \tag{4-9}$$

Express Equation (4-9) as;

$$A \times C = B \tag{4-10}$$

Least Square approach uses the following equation to compute Thevenin equivalent source voltage and impedance.

$$C = (A^{'}A)^{-1} A^{'} B \tag{4-11}$$

In this study, we used 4 measurement points as a sliding window to continuously track the Thevenin Equivalent. Least Square approach is based on the assumption that the Thevenin Equivalent value will remain unchanged during the measurement time period. The accuracy of Least Square approach will be degraded if there is a dramatic change of network topology.

4.4 Estimation of the Thevenin Equivalent using Kalman Filter Method

Kalman Filter is a set of mathematical equations that provides an efficient computational (recursive) means to estimate the state of a process, in a way that minimizes the mean of the squared error. Kalman Filter is very powerful in two aspects:

- It supports estimations of past, present and even future states
- It can do so even when the precise nature of the modeled system is unknown [6].

Assume the estimation equation is:

$$\hat{z} = H\hat{x} + \hat{v} \tag{4-12}$$

where $\hat{z}$ is the measurement vector. $\hat{x}$ is the state vector to be estimated, and H is the observation model. $\hat{v}$ is the observation noise.

To minimize the estimation error, we are trying to minimize a cost function that

$$J = \frac{1}{2}(\hat{z} - H\hat{x})^T (\hat{z} - H\hat{x}) \tag{4-13}$$

The criterion to minimize the J is that its derivative equals to zero

$$\frac{\partial J}{\partial \hat{x}} = -(\hat{z} - H\hat{x})^T H = 0 \tag{4-14}$$

At that time the estimation of $\hat{x}$ is given as

$$\hat{x}_{est} = (H^T H)^{-1} H^T \hat{z} \tag{4-15}$$

Now deriving a recursive equation to estimate the $\hat{x}$. Let P be the covariance of the error in the estimator as

$$\begin{aligned} P &= E\left[\tilde{x}_{est}\tilde{x}_{est}{}^T\right] \\ &= (H^T H)^{-1} H^T R H (H^T H)^{-1} \\ &= (H^T R^{-1} H)^{-1} \end{aligned} \tag{4-16}$$

where $\tilde{x}_{est} = x - \hat{x}_{est}$, R is the covariance matrix of measurement error.

Represent Equation (4-16) using the samples, we get

$$\begin{aligned} P_n &= (\sum_{i=1}^{n} H_i^{\,T} R_i^{-1} H_i)^{-1} \\ &= (\sum_{i=1}^{n-1} H_i^{\,T} R_i^{-1} H_i + H_n^{\,T} R_n^{-1} H_n)^{-1} \\ &= (P_{n-1}^{\;-1} + H_n^{\,T} R_n^{-1} H_n)^{-1} \end{aligned} \tag{4-17}$$

If consider R as a weighting matrix, Equation (4-15) at time instant n can be written as

$$\begin{aligned} \hat{x}_n &= (\sum_{i=1}^{n} H_i^{\,T} R_i^{-1} H_i)^{-1} (\sum_{i=1}^{n} H_i^{\,T} R_i^{-1} z_i) \\ &= P_n \left[\sum_{i=1}^{n-1} H_i^{\,T} R_i^{-1} z_i + H_n^{\,T} R_n^{-1} z_n \right] \\ &= P_n (P_{n-1}^{\;-1} \hat{x}_{n-1} + H_n^{\,T} R_n^{-1} z_n) \end{aligned} \tag{4-18}$$

Define

$$K_n = P_n H_n^T R_n^{-1} \tag{4-19}$$

Then Equation (4-18) will be

$$\hat{x}_n = P_n P_{n-1}^{-1} \hat{x}_{n-1} + K_n \hat{z}_n \tag{4-20}$$

Since

$$P_n P_{n-1}^{-1} = I - K_n H_n \tag{4-21}$$

Then, the recursive equation to estimate $\hat{x}_n$ is

$$\hat{x}_n = \hat{x}_{n-1} + K_n [z_n - H_n \hat{x}_{n-1}] \tag{4-22}$$

Now apply the above method in our load shedding problem. From Fig. 3-1, we can see

$$E - jY^{-1} I = V \tag{4-23}$$

where,

V and I are from the measurements from the local relay;

Denote $E = E_r + jE_i$, $V = m + jn$, $I = p + jq$, $Z = 1/Y = R + jX$.

Then, in according with Equation (4-12), we have

$$\hat{z} = \begin{bmatrix} m \\ n \end{bmatrix} \tag{4-24}$$

$$H = \begin{bmatrix} 1 & 0 & -p & q \\ 0 & 1 & -q & -p \end{bmatrix} \tag{4-25}$$

$$\hat{\mathrm{x}} = \begin{bmatrix} \mathrm{E_r} \\ \mathrm{E_i} \\ \mathrm{R} \\ \mathrm{X} \end{bmatrix} \tag{4-26}$$

When applying the recursive Equation (4-22), several parameters need to be initialized. Based on our studies, we suggest that the initial value of $\hat{x}$ is set based on the calculated Thevenin Equivalent in base case power flow. For the covariance matrix of measurement error R, it can be obtained from the accuracy of the measurement device. In this study, we set it as a diagonal matrix with the element value equal to 0.01. For covariance matrix of the estimator error P, we set the initial value of P as a diagonal matrix with the element value equal to 0.00001.

We set the sampling rate as 0.01s or 1 cycle based on 60Hz. It is set based on consideration of calculation as well as providing enough time to detect a fault then block the load shedding function during the fault. To continuously track the Thevenin Equivalent using Kalman Filter, we use four measurement samples as a sliding window.

4.5 Comparison between the Least Square and Kalman Filter Approaches

For Least Square approach, it makes use of measurements taken at different time instant to estimate the equivalent source voltage and impedance. Please note that this is primarily based on the assumption that there will be no change of the Thevenin equivalent between the measurements taken at different time steps. Otherwise, the accuracy of this technique may be questionable. Moreover, at each time instant, the calculation will repetitively involve the calculation for inverse matrix for the entire updated data window. The convergence rate is relatively slow.

However, Kalman Filter approach proposed in this invention derives a recursive set of equations for state estimation. When the new measurements are fed in, the calculation only updates the K_n in Equation (4-22). The calculations in the previous steps will still have a contribution to the final true value of the estimated vector. It usually has a fast convergence rate hence it is suitable for on-line application.

In order to compare the two estimation techniques, numerous steady state and dynamic simulations have been conducted. Section 4.5.1 will show the results of steady state simulations. Section 4.5.2 will show the study results of dynamic simulations.

4.5.1 Comparison between Least Square Approach and Kalman Filter Approach based on Steady State Simulation

The simulations are based on the IEEE 39 bus system. For the steady state simulation, the iterative power flow is used to simulate the voltage collapse phenomenon. The load at bus 26 increases until voltage instability reaches.

- The load at bus 26 increases 10 MW per step.
- Reactive power increases correspondingly according to the base case P/Q ratio.
- Governor power flow is used to calculated generators' output in order to balance the increasing load.
- Generator reactive power output limits are also considered.
- The simulation ends when the power flow calculation failed to converge.

Figure 4-1 and Figure 4-2 show the steady state simulation results. The red line shows the apparent impedance of load. The pink line shows the calculated Thevenin impedance. The blue line shows the estimated Thevenin impedance using Least Square approach. The black line shows the estimated Thevenin impedance using Kalman Filter approach. We can see that both Least Square approach and Kalman Filter approach produce the estimation results close to the actual Thevenin Equivalent. In comparison, Kalman Filter approach provides more accurate results than Least Square approach.

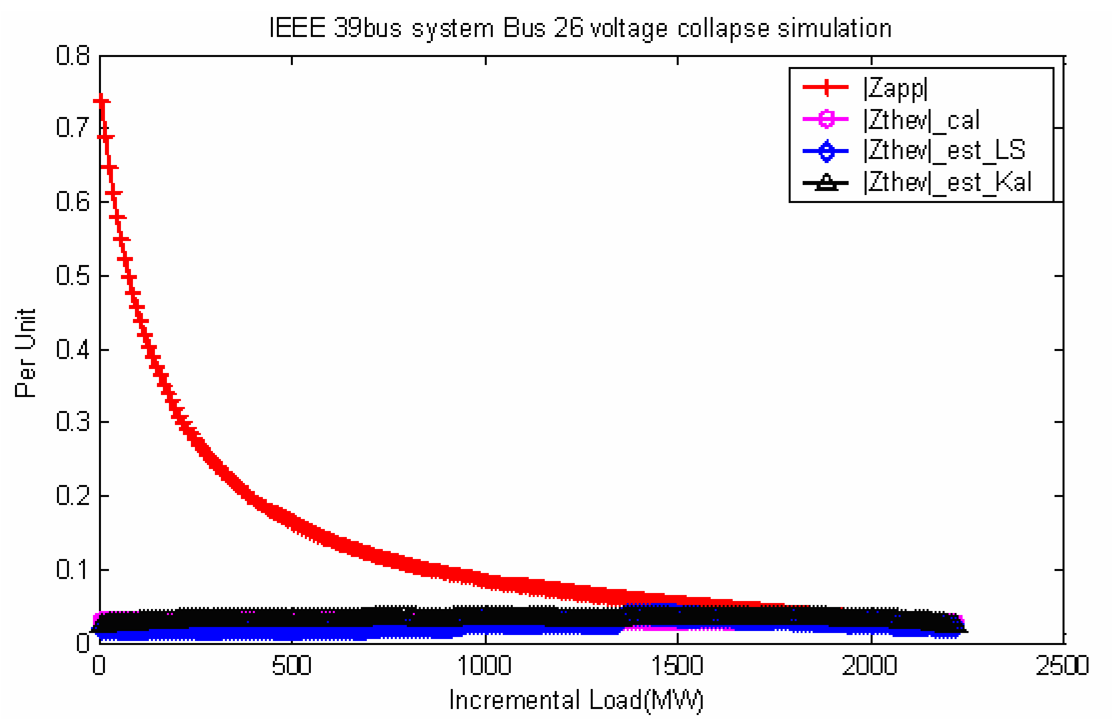

Figure 4-1
Estimation results of Thevenin Equivalent in steady state simulation

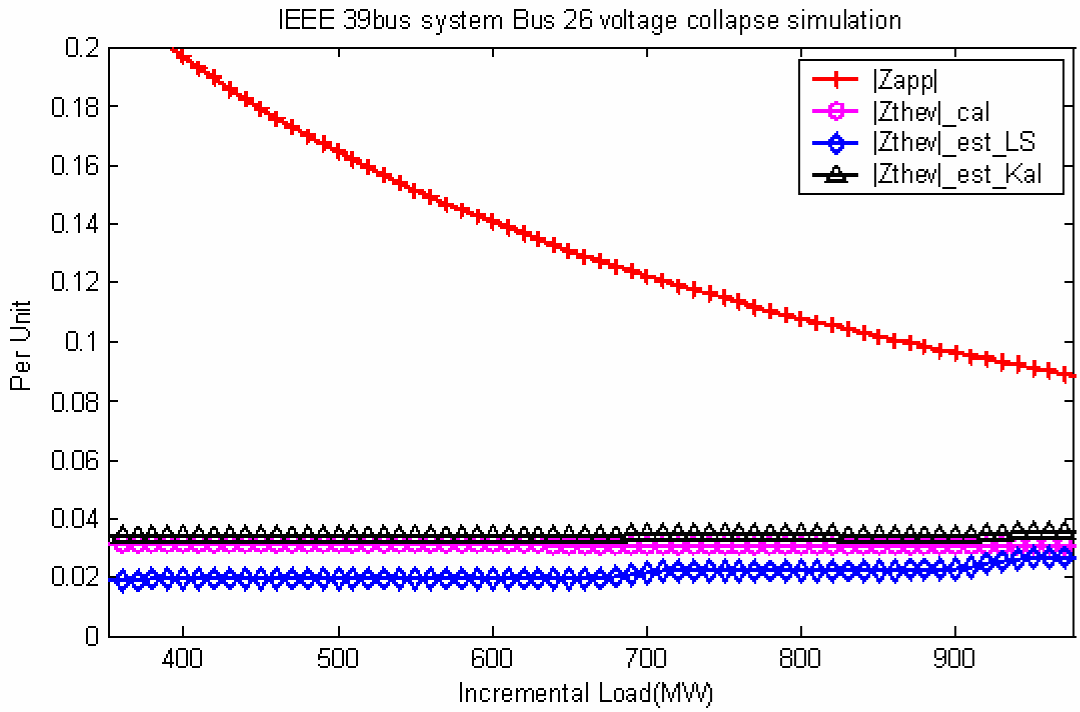

Figure 4-2
Estimation results of Thevenin Equivalent (Zoomed Area) in steady state simulation

4.5.2 Comparison between Least Square Approach and Kalman Filter Approach based on Dynamic Simulation

Dynamic simulation is performed to compare the accuracy of these two estimation methods. In the dynamic simulation, generators' exciters and governors have been modeled. We gradually increase the load at Bus 26 of IEEE 39-bus system at a rate of 50MW and 6.7Mvar per second. Figure 4-3 shows the current and voltage magnitudes at bus 26.

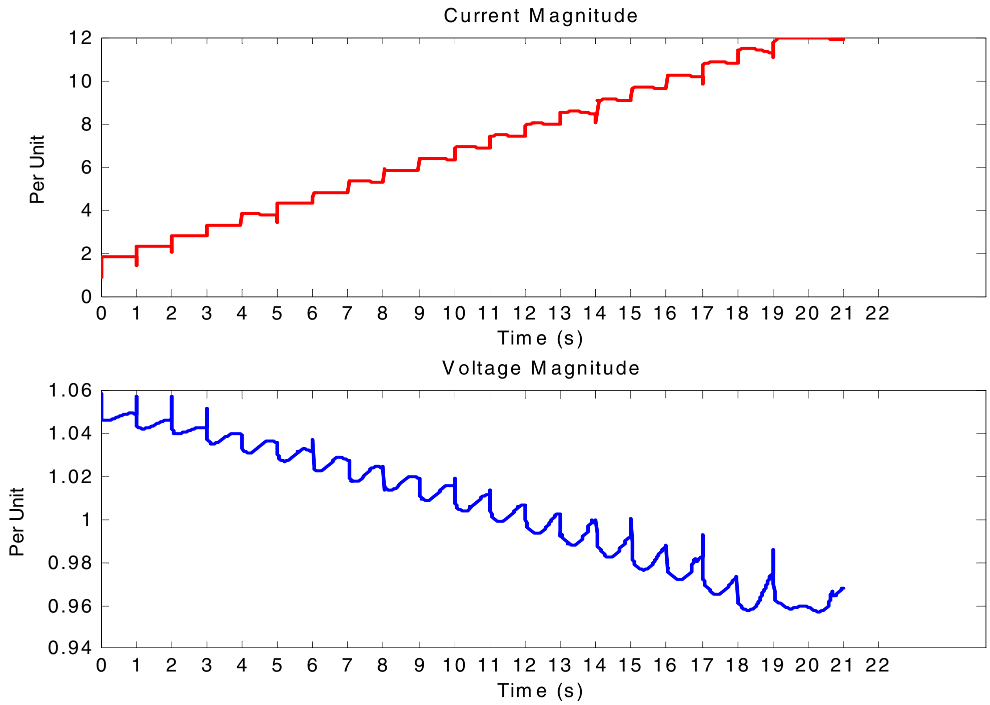

Figure 4-3
Current and voltage profile during dynamic simulation

Figure 4-4 and Figure 4-5 show the estimation results. We can see that the estimation value using the Least Square approach is incorrect. The estimated values when there is no load change are totally incorrect. This confirms that the Least Square approach is effective only when the system condition is changing. In contrast, the Kalman Filter based estimation method produces much more accurate results.

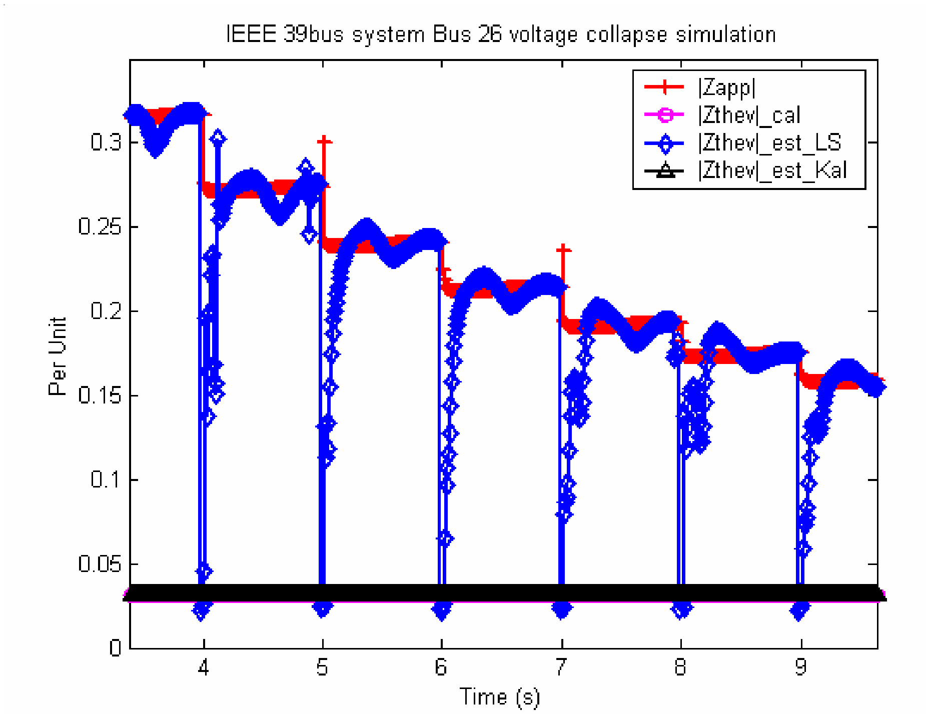

Figure 4-4
Estimation results of Thevenin Estimation in dynamic simulation

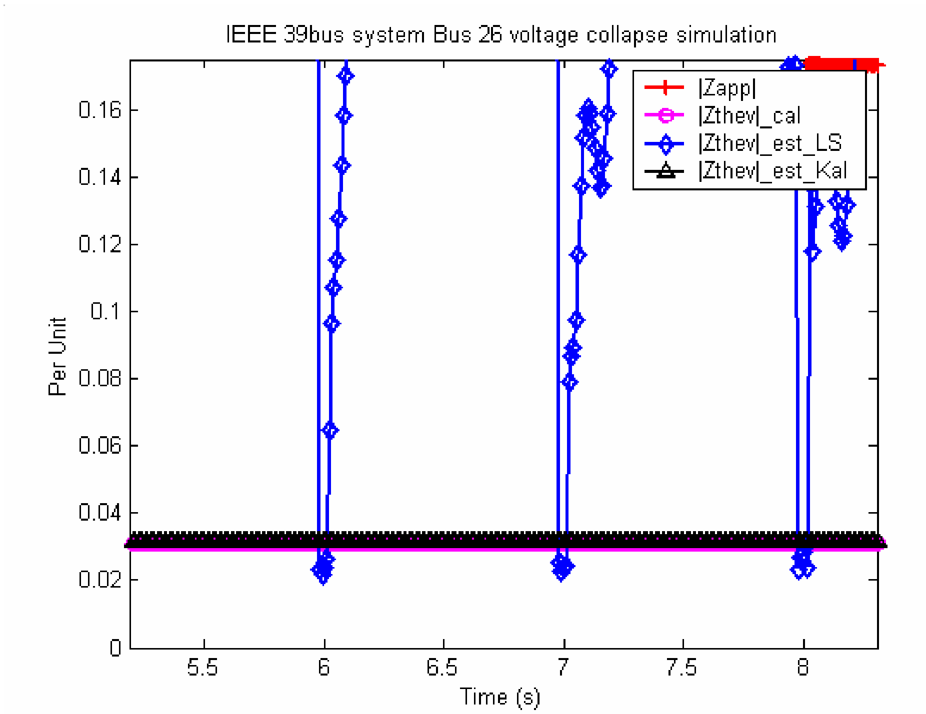

Figure 4-5
Estimation results of Thevenin Equivalent (Zoomed Area) in dynamic simulation

We also compared Least Square approach and Kalman Filter approach during transient stages. Three phase fault at the end of line 29-26 is simulated at 1.0s and the line 29-26 is tripped at 1.1s to clear the fault. Figure 4-6 shows the current and voltage magnitudes at bus 26.

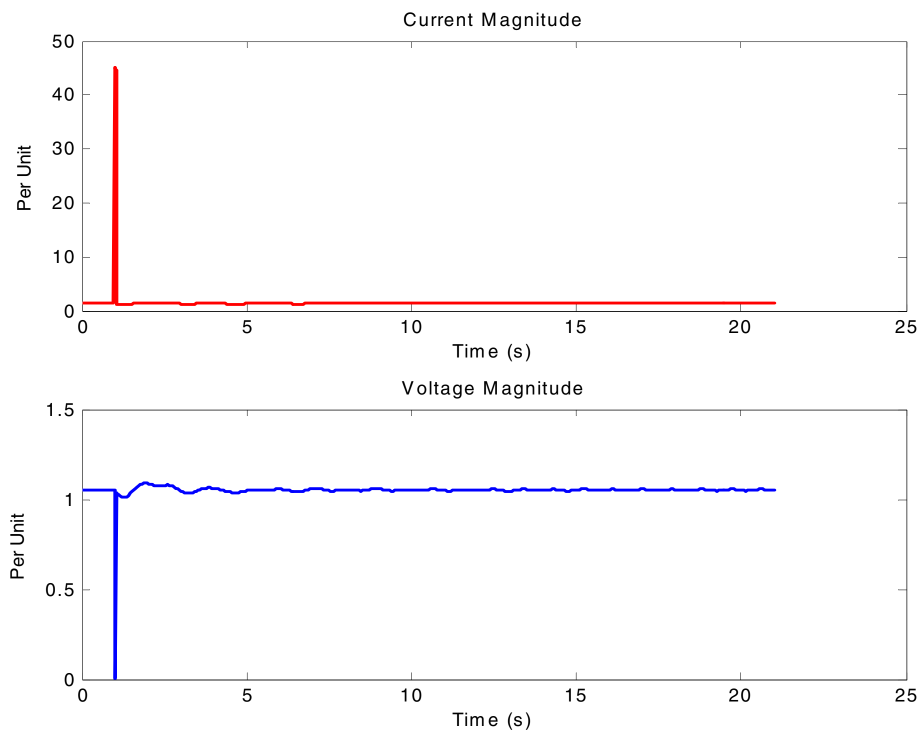

Figure 4-6
Current and voltage profile during fault at bus 26

Figure 4-7 and Figure 4-8 show that Kalman Filter approach can produce much closer estimation results to the actual Thevenin Equivalent compared with the Least Square approach.

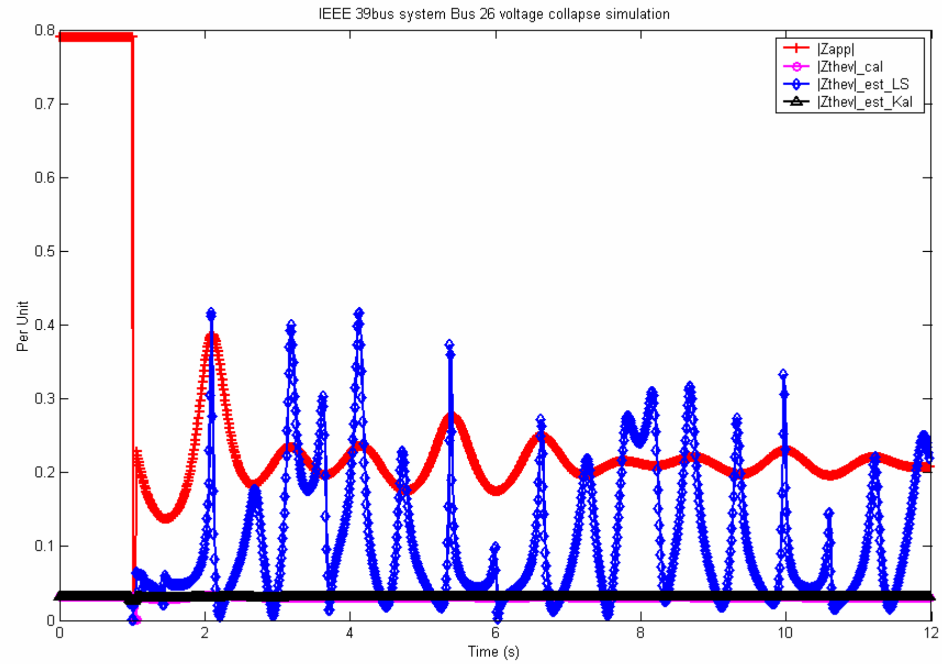

Figure 4-7
Estimation results for Thevenin Equivalent during fault

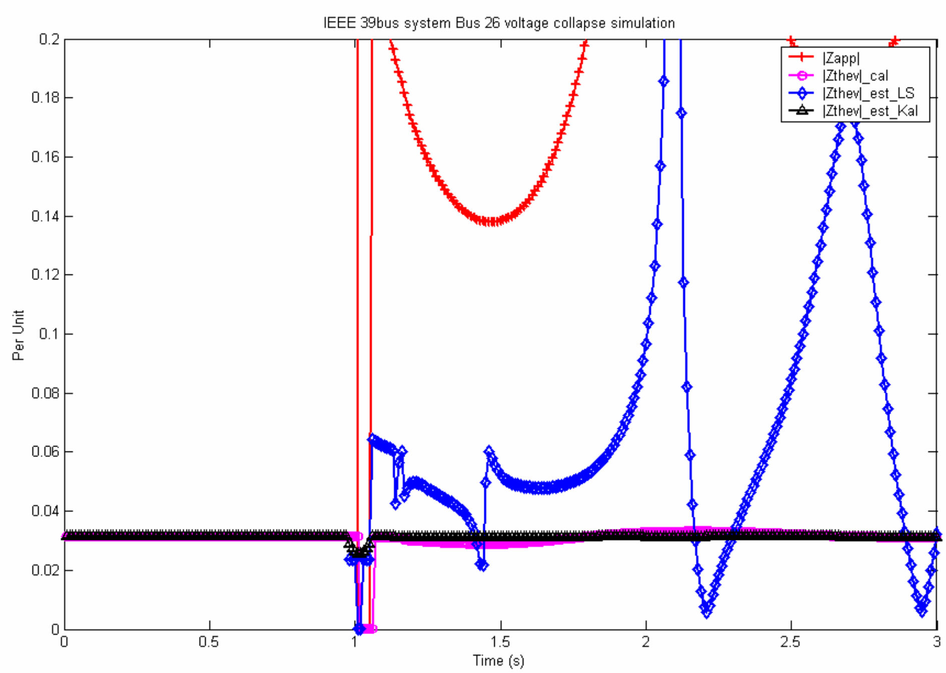

Figure 4-8
Estimation results for Thevenin Equivalent during fault (Zoomed Area)

In summary,

- For steady state simulation, both Least Square approach and Kalman Filter approach can produce accurate result.
- During small disturbances, Kalman Filter approach produces more accurate results than Least Square approach.
- The study results confirm that load shedding scheme should be blocked during fault.

5 SUMMARY AND FUTURE WORK

5.1 Summary

A new control scheme referred as “Voltage Instability Load Shedding” (VILS) is disclosed in this report to enhance the conventional UVLS at designated location, such as major load centers. The VILS control scheme uses local measurements to continuously compute Voltage Stability Margin Index (VMSI) to track voltage stability margin at local bus level. The VMSI is expressed in terms of active, reactive and apparent power, which indicates how much load to be shed to bring the system back to voltage stable region. When this smart device detects that the voltage stability conditions cross a warning threshold, it will send an alarm signal to inform system operators. When it detects that the voltage stability conditions cross an emergency level, it will perform local load shedding function.

VILS method also has two advantages over the VIP method.

- The VIP method uses the Least Square technique to determining the Thevenin equivalent source impedance. The Least Square method makes use of measurements taken at different time instant to estimate the equivalent source impedance.. Least square approach is based on the assumption that the Thevenin Equivalent value will remain unchanged during the measurement time period. The accuracy of Least Square approach will be degraded if there is a dramatic change of network topology. The VILS uses Kalman Filter technique to track Thevenin Equivalent which is a recursive method that has the fast convergence property, Time domain simulation results clearly indicates that Kalman Filter method provides more accurate results than Least Square method.
- The VIP method propose using the closeness between the the apparent load impedance and the equivalent Thevenin impedance to initiate load shedding, which can not provide and the information of how much load should be shed. The VILS method uses VSMI as the triggering criteria to shed load. The VMSI is expressed in terms of active, reactive and apparent power, which indicates clearly how much load to be shed to bring the system back to voltage stable region.

5.2 Future Work

In terms of near-term future work, we will focus on the validation of VILS using field measurement data. We will also develop the special protection relay using VILS control scheme and demonstrate the effectiveness of this device through field installation and test.

In term of long-term future work, we will install VILS devices across the entire transmission network and develop the visualization tool to help system operators to monitor system voltage stability conditions. We will also investigate and develop control algorithms at control center level to use the real-time data collected from VILS devices and EMS system to control system voltage stability margin and initiate coordinated load shedding to prevent wide-area voltage collapse.

6 REFERENCES

1. Taylor, C.W., Power System Voltage Stability, McGraw Hill, 1994
2. TUAN, T.Q., FANDINO, J., HADJSAID, N., SABONNADIERE, J.C., and VU, H.: 'Emergency load shedding to avoid risks of voltage instability using indicators', ZEEE Truns., 1994, HL9, (1). pp. 341-351.
3. TSO, S.K., ZHU, T.X., ZENG, Q.Y., and LO, K.L.: 'Evaluation of load shedding to prevent dynamic voltage instability based on extended fuzzy reasoning', IEE Proc., Gener. Transm. Distrib.,1997, 144, (2),'pp. 81- 86.
4. ARNBORG, S . , ANDERSON, C., HILL, D.J., and HISKENS, LA.: 'On undervoltage load shedding in power svstems', Int. J. Elect. Power Energy &st., 1997, 19, @), pp. 141- 149
5. Khoi Vu, Miroslav M. Begovic, Damir Novosel, and Murari Mohan Saha, "Use of Local Measurements to Estimate Voltage-Stability Margin," *IEEE Transactions on Power Systems*, vol. 14, no. 3, August 1999.
6. Greg Welch and Gary Bishop, "An Introduction to the Kalman Filter", TR 95-041, University of North Carolina, Department of Computer Science, April, 2004

Export Control Restrictions

Access to and use of EPRI Intellectual Property is granted with the specific understanding and requirement that responsibility for ensuring full compliance with all applicable U.S. and foreign export laws and regulations is being undertaken by you and your company. This includes an obligation to ensure that any individual receiving access hereunder who is not a U.S. citizen or permanent U.S. resident is permitted access under applicable U.S. and foreign export laws and regulations. In the event you are uncertain whether you or your company may lawfully obtain access to this EPRI Intellectual Property, you acknowledge that it is your obligation to consult with your company's legal counsel to determine whether this access is lawful. Although EPRI may make available on a case-by-case basis an informal assessment of the applicable U.S. export classification for specific EPRI Intellectual Property, you and your company acknowledge that this assessment is solely for informational purposes and not for reliance purposes. You and your company acknowledge that it is still the obligation of you and your company to make your own assessment of the applicable U.S. export classification and ensure compliance accordingly. You and your company understand and acknowledge your obligations to make a prompt report to EPRI and the appropriate authorities regarding any access to or use of EPRI Intellectual Property hereunder that may be in violation of applicable U.S. or foreign export laws or regulations.

The Electric Power Research Institute (EPRI)

The Electric Power Research Institute (EPRI), with major locations in Palo Alto, California, and Charlotte, North Carolina, was established in 1973 as an independent, nonprofit center for public interest energy and environmental research. EPRI brings together members, participants, the Institute's scientists and engineers, and other leading experts to work collaboratively on solutions to the challenges of electric power. These solutions span nearly every area of electricity generation, delivery, and use, including health, safety, and environment. EPRI's members represent over 90% of the electricity generated in the United States. International participation represents nearly 15% of EPRI's total research, development, and demonstration program.

Together…Shaping the Future of Electricity

Printed on recycled paper in the United States of America

1012491

ELECTRIC POWER RESEARCH INSTITUTE

3420 Hillview Avenue, Palo Alto, California 94304-1395 • PO Box 10412, Palo Alto, California 94303-0813 • USA
800.313.3774 • 650.855.2121 • askepri@epri.com • www.epri.com